arXiv:0812.2821v2 [hep-ph] 4 Apr 2009

High density quark matter in the NJL model with dimensional vs. cut-off regularization

T. Fujihara, D. Kimura
Department of Physics, Hiroshima University, Higashi-Hiroshima, Hiroshima 739-8526, JAPAN

T. Inagaki
Information Media Center, Hiroshima University,
Higashi-Hiroshima, Hiroshima 739-8521, JAPAN

A. Kvinikhidze
A. Razmadze Mathematical Institute of Georgian Academy of Sciences, M. Alexidze Str. 1, 380093 Tbilisi, Georgia

(Dated: April 6, 2009)

We investigate color superconducting phase at high density in the extended Nambu–Jona-Lasinio model for the two flavor quarks. Because of the non-renormalizability of the model, physical observables may depend on the regularization procedure, that is why we apply two types of regularization, the cut-off and the dimensional one to evaluate the phase structure, the equation of state and the relationship between the mass and the radius of a dense star. To obtain the phase structure we evaluate the minimum of the effective potential at finite temperature and chemical potential. The stress tensor is calculated to derive the equation of state. Solving the Tolman-Oppenheimer-Volkoff equation, we show the relationship between the mass and the radius of a dense star. The dependence on the regularization is found not to be small, interestingly, dimensional regularization predicts color superconductivity phase at rather large values of μ (in agreement with perturbative QCD in contrast to the cut-off regularization), in the larger temperature interval, the existence of heavier and larger quark stars.

PACS numbers: 11.10.Kk, 11.30.Qc, 12.39.-x

I. INTRODUCTION

Variety of new phases of the matter consisting of quarks and gluons is expected in the high density QCD. One of them is the broken color $SU_c(3)$ symmetry phase where the color superconductivity takes place, Refs. [1-4] Quark-quark interaction is attractive in the color anti-symmetric $\bar{3}$ channel. This force destabilizes the filed Fermi sea leading to the Cooper instability. Then a composite operator constructed from a color anti-triplet diquark pair develops a non-vanishing expectation value. For the case of the two flavor quarks the diquark condensation breaks the color $SU_c(3)$ symmetry down to the $SU_c(2)$. This broken symmetry phase is called two-flavor color superconducting (2SC) phase. Because of the high degeneracy of states near the Fermi surface, such a symmetry breakdown behavior is a subject of a non-perturbative description in QCD.

To investigate non-perturbative QCD effects we are working in the low energy effective theory, namely in the Nambu–Jona-Lasinio (NJL) model in which the chiral symmetry is broken down dynamically [5]. The model is useful to evaluate low-energy phenomena in hadronic phase of QCD. The NJL model is extended in a simple way to include the attraction in the $\bar{3}$ qq channel. It is based on the point-like four-fermion interactions between quarks. Since the four-fermion interaction is the dimension 6 operator, the model is non-renormalizable in four space-time dimensions, therefore some regularization is needed to obtain finite results.

Most of analysis have been using momentum cut-off regularization, where the cut-off scale is determined phenomenologically. Unfortunately this cut-off scale often breaks some symmetries of the model. Moreover the critical chemical potential where the color superconductivity takes place is of the order of the cut-off scale (ultraviolet cut-off may even hit the Fermi sea cut-off). In such a situation, it is expected that the regularization procedure has a non-negligible effect on the analysis of the color superconductivity. That is why in the present paper we analyze the extended NJL model by using the dimensional regularization as well. In the dimensional regularization the space-time dimension is analytically continued to less than four.

Some high density states are observed in astrophysical objects. In the core of dense stars, like neutron stars interior, quark stars and so on, the color superconducting phase is expected to take place. Much attention has been paid to such dense stars to find an evidence of the color superconductivity [6, 7]. Characteristics of the dense stars such as the mass and the radius are of great interest. A constraint on the mass and the radius of the star can be found by solving the Tolman-Oppenheimer-Volkoff (TOV) equation [8]. This solution depends on the equation of state (EoS), i.e. on the relationship between the energy density and the pressure, of the quark matter inside the stars. It was pointed out that the existence of the color superconducting phase may decrease the minimum of the radius of such dense stars [6, 7], [9-29].The minimal size of the stars is analyzed precisely.

A finite contribution from the color neutrality and the β equilibrium are analyzed in [11-15]. Nucleon and vector meson contributions are calculated in [16-19]. Rotating compact stars are considered in [20].

In the paper the extended NJL model is regarded as a low energy effective theory of QCD. We consider two flavor quarks and investigate properties of compact stars in the 2SC phase. In Sec. II we introduce the model Lagrangian and the fermion propagator in color superconducting phase. In Sec. III the phase structure of the model is evaluated at finite temperature and chemical potential. We numerically calculate expectation values of the composite operators $\langle\bar{\psi}\psi\rangle$ and $\langle\overline{\psi^c}\psi\rangle$ and the quark number susceptibility. In Sec. IV we evaluate the energy-momentum tensor and determine the EoS . In Sec. V we solve the TOV equation with the account of the obtained EoS and show the relationship between the radius and the mass of a dense star in the color superconducting phase. Finally we give concluding remarks.

II. EXTENDED NJL MODEL

In a state with large chemical potential the $\bar{3}$ diquark channel interaction plays essential role in creation of a color Cooper pair of quarks. To study color superconductivity one can extend the NJL model to include the $\bar{3}$ diquark interactions explicitly. The temperature, T, and the chemical potential, μ, is introduced to the theory via the imaginary time formalism. The model is defined by the Lagrangian density

$$\begin{aligned}\mathcal{L} &= \bar{\psi}(i\partial\!\!\!/ - m - i\mu\gamma_4)\psi \\ &\quad + G_S\{(\bar{\psi}\psi)^2 + (\bar{\psi}_{aj}i\gamma_5\boldsymbol{\tau}_{jk}\psi_{ak})^2\} \\ &\quad + G_D(i\overline{\psi^c}_{aj}\varepsilon_{jk}\epsilon^b_{ad}\gamma_5\psi_{dk})(i\bar{\psi}_{fl}\varepsilon_{lm}\epsilon^b_{fg}\gamma_5\psi^c{}_{gm}),\end{aligned} \tag{1}$$

where the indices a, b, d, e, f, g and j, k, l, m denote the colors(1,2,3) and flavors(u, d) of the quarks, m is the quark mass matrix, diag(m_u, m_d), $\boldsymbol{\tau}_{jk}$ represents the isospin Pauli matrices, ψ^c is the charge conjugate of the field ψ. G_S and G_D are the effective coupling constants for the $q\bar{q}$ scalar and the diquark channel respectively. The third line in Eq. (1) exposes the attractive force in the $\bar{3}$ channel of the quark-quark interaction.

For practical calculations it is convenient to introduce the auxiliary fields: scalar σ, pseudo-scalar $\boldsymbol{\pi}$ and diquark Δ^b, to write down the Lagrangian density as

$$\mathcal{L}_{\text{aux}} = \frac{1}{2}\bar{\Psi}G^{-1}\Psi - \frac{1}{4G_S}(\sigma^2 + \boldsymbol{\pi}^2) - \frac{1}{4G_D}|\Delta^b|^2, \tag{2}$$

where the Nambu-Gor'kov representation [35] is used,

$$\Psi = \begin{pmatrix} \psi \\ \psi^c \end{pmatrix}, \tag{3}$$

and G represents the quark propagator,

$$G^{-1} \equiv \begin{pmatrix} i\partial\!\!\!/ - m - i\mu\gamma_4 - \sigma - i\gamma_5\boldsymbol{\pi}\cdot\boldsymbol{\tau} & -i\Delta^a\varepsilon\epsilon^a\gamma_5 \\ -i\Delta^{b*}\varepsilon\epsilon^b\gamma_5 & i\partial\!\!\!/ - m + i\mu\gamma_4 - \sigma - i\gamma_5\boldsymbol{\pi}\cdot\boldsymbol{\tau}^T \end{pmatrix}. \tag{4}$$

From the equation of motion for the auxiliary fields we get the following correspondence,

$$\sigma \sim -G_S\bar{\psi}\psi, \tag{5}$$

$$\boldsymbol{\pi} \sim -G_S\bar{\psi}i\gamma_5\boldsymbol{\tau}\psi, \tag{6}$$

$$\Delta^b \sim -G_D i\overline{\psi^c}_{aj}\varepsilon_{jk}\epsilon^b_{ad}\gamma_5\psi_{dk}. \tag{7}$$

The generating functional for the Lagrangian density (2) is given by

$$\begin{aligned} Z &= \int \mathcal{D}(\Psi, \bar{\Psi}, \Delta^b, \Delta^{b*}, \sigma, \boldsymbol{\pi}) e^{\int d^4x\left(\mathcal{L}_{\text{aux}} - \frac{1}{2}\bar{\Psi}\cdot J_{\bar{\Psi}} - \frac{1}{2}J_\Psi\cdot\Psi\right)} \\ &= \mathcal{N}\int \mathcal{D}(\Delta^b, \Delta^{b*}, \sigma, \boldsymbol{\pi}) \det{}^{1/2}G^{-1} \\ &\quad \times\exp\left[-\int d^4x\ \left(\frac{\sigma^2 + \boldsymbol{\pi}^2}{4G_S} + \frac{|\Delta^b|^2}{4G_D}\right)\right. \\ &\quad \left. - \frac{1}{2}\int d^4x d^4y\ J_\Psi(x)G(x-y)J_{\bar{\Psi}}(y)\right], \end{aligned} \tag{8}$$

where $\mathcal{N}$ is a constant and the sources are

$$J_{\bar{\Psi}} \equiv \begin{pmatrix} J_{\bar{\psi}} \\ J_{\overline{\psi^c}} \end{pmatrix}, \quad J_\Psi \equiv (J_\psi, J_{\psi^c}). \tag{9}$$

The quark mass affects the scalar σ channel [36], we set $\boldsymbol{\pi} = \mathbf{0}$. $SU_c(3)$ symmetry allows one to set $\Delta^{1,2} = 0$ and $\Delta \equiv \Delta^3$. Here we study the phase structure for the case of the two flavor quarks.

III. PHASE STRUCTURE

The phase structure is determined by the effective potential. We set $J_\Psi = J_{\bar{\Psi}} = 0$ in the generating functional (8) to obtain the effective potential,

$$V_{\text{eff}}(\sigma, \Delta) = \frac{\sigma^2}{4G_S} + \frac{\Delta^2}{4G_D} - \frac{1}{2\beta\Omega}\ln\det\left(G^{-1}\right). \tag{10}$$

where Ω denotes the volume of the system, $\Omega \equiv \int d^{D-1}x$. Due to the space-time translational invariance the expectation values of σ and Δ are independent of the space-time coordinates. Assuming the isospin symmetry, $m_u = m_d = m$ and $\mu_u = \mu_d = \mu$, the effective potential reads

$$\begin{aligned} V_{\text{eff}}(\sigma, \Delta) &= \frac{1}{4G_S}\sigma^2 + \frac{1}{4G_D}\Delta^2 \\ &\quad - \text{tr}\mathbf{1}_{\text{spinor}}\int\frac{d^{D-1}p}{(2\pi)^{D-1}}\left[E_+ + E_- + E\right. \\ &\quad + 2\frac{1}{\beta}\ln\left\{(1 + e^{-\beta E_+})(1 + e^{-\beta E_-})\right\} \\ &\quad \left. + \frac{1}{\beta}\ln\left\{(1 + e^{-\beta\xi_+})(1 + e^{-\beta\xi_-})\right\}\right], \end{aligned} \tag{11}$$

where $\text{tr}\mathbf{1}_{\text{spinor}} = 2^{D/2}$, $\beta = 1/T$ and

$$E \equiv \sqrt{\boldsymbol{p}^2 + (\sigma + m)^2},\ \xi_\pm \equiv E \pm \mu,\ E_\pm \equiv \sqrt{\xi_\pm^2 + \Delta^2}. \tag{12}$$

Since the third term of the right hand side of Eq. (11) involves a divergent integral, we use the dimensional regularization ($2 < D < 4$) to regularize it [37, 38]. After integration over the angle variables, we have

$$\begin{aligned} V_{\rm eff}(\sigma,\Delta) &= \frac{\sigma^2}{4G_S}+\frac{\Delta^2}{4G_D}-\frac{\tilde{A}}{\Gamma\left(\frac{D-1}{2}\right)} \\ &\quad\times\int_0^\infty dp\, p^{D-2}\left[E_+ + E_- + E\right. \\ &\quad+2\frac{1}{\beta}\ln(1+e^{-\beta E_+})+2\frac{1}{\beta}\ln(1+e^{-\beta E_-}) \\ &\quad\left.+\frac{1}{\beta}\ln(1+e^{-\beta\xi_+})+\frac{1}{\beta}\ln(1+e^{-\beta\xi_-})\right], \end{aligned} \tag{13}$$

with $\tilde{A} \equiv 4\sqrt{\pi}/(2\pi)^{D/2}$. For the cut-off regularization, the third term of the right hand side is obtained by the replacement

$$\frac{\tilde{A}}{\Gamma\left(\frac{D-1}{2}\right)}\int_0^\infty dp\, p^{D-2} \to \frac{2}{\pi^2}\int_0^\Lambda dp\, p^2, \tag{14}$$

where Λ is a cut-off scale. The first three terms of the integral in Eq. (13) are naively divergent. The divergent part of the Eq. (13) in the dimensional regularization reads

$$\begin{aligned} &\int_0^\infty dp\, p^{D-2}\,(E_+ + E_- + E) \\ &= \int_0^\infty dp\, p^{D-2}\left(E_+ + E_- - 2\sqrt{E^2+\Delta^2}\right) \\ &\quad-\frac{\Gamma(-\frac{D}{2})\Gamma(\frac{D-1}{2})}{4\sqrt{\pi}}\left[2\{(\sigma+m)^2+\Delta^2\}^{D/2}\right. \\ &\quad\left.+\{(\sigma+m)^2\}^{D/2}\right]. \end{aligned} \tag{15}$$

The following renormalization conditions are used:

$$\begin{aligned} \frac{1}{2G_S^r} &= \left.\frac{\partial^2 V_{\rm eff}}{\partial\sigma\partial\sigma}\right|_{\mu=T=\Delta=0,\sigma=M_0} \\ &= \frac{1}{2G_S} \\ &\quad+\frac{3D(D-1)}{(2\pi)^{D/2}}\Gamma\left(-\frac{D}{2}\right)\left[(M_0+m)^2\right]^{D/2-1} \end{aligned} \tag{16}$$

and

$$\begin{aligned} \frac{1}{2G_D^r} &= \left.\frac{\partial^2 V_{\rm eff}}{\partial\Delta\partial\Delta}\right|_{\mu=T=\Delta=0,\sigma=M_0} \\ &= \frac{1}{2G_D} \\ &\quad+\frac{2D}{(2\pi)^{D/2}}\Gamma\left(-\frac{D}{2}\right)\left[(M_0+m)^2\right]^{D/2-1}, \end{aligned} \tag{17}$$

where M_0 is a renormalization scale.

The parameters of the model are fixed to reproduce some observables at $T = \mu = 0$. Using the pion mass $m_\pi = 138$ MeV, the pion decay constant $f_\pi = 92.4$ MeV and the quark mass $m = 4.5$ MeV, we obtain $\Lambda = 720$ MeV and $G_S = 3.80 \times 10^{-6}$ MeV^{-2} for the cut-off regularization. Here we use the relationship, $G_D = (3/4)G_S$, corresponding to the one gluon exchange interaction. In the chiral limit, the critical temperature becomes 170 MeV at $\mu = 0$ with these parameters.

In the dimensional regularization one can not avoid renormalization which introduces an additional parameter, renormalization scale, M_0. In Ref. [37] the scale is simply fixed at the dynamically generated fermion mass. The similar procedure is also adopted in [39]. Here we fix all parameters by reproducing physical observables. Reproduction of the critical temperature places an additional constraint on the parameters. We fix the parameters for the dimensional regularization to reproduce the pion mass, the pion decay constant, the quark mass and the critical temperature 170 MeV at $m \to 0$ and $\mu = 0$. Then we have $D = 2.28$, $M_0 = 127$ MeV, $G_S^r = 0.603$ MeV^{2-D} and $G_D^r = (3/4)G_S^r$ for the dimensional regularization. In Ref. [40] the renormalization scale is fixed by using the decay width of the $\pi^0 \to 2\gamma$. It gives the renormalization scale near the constituent quark mass.

If the auxiliary field $\Delta \equiv \Delta^3$ develops a non-vanishing value, the diquark condensation takes place. It implies that the QCD gauge symmetry is broken down from $SU_c(3)$ to $SU_c(2)$ and the 2SC phase is realized. The expectation values of σ and Δ are found by observing the minimum of the effective potential. To find the minimum we numerically evaluate the effective potential (13). The expectation values are shown as functions of the chemical potential in Figs. 1 and 2 near a typical temperature of dense star, $T = 1$ keV, in the cut-off and the dimensional regularizations respectively. We observe similar behavior of $\langle\sigma\rangle$ and $\langle\Delta\rangle$ in Figs. 1 and 2. As is known, the current quark mass enhances the chiral symmetry breaking and contributes to the crossover behavior, i.e. the expectation value, $\langle\sigma\rangle$, smoothly disappears as the

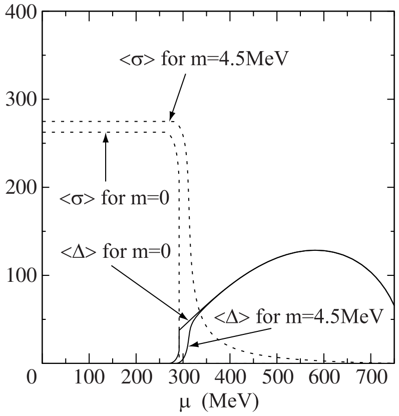

FIG. 1: Behavior of the expectation values of auxiliary fields σ and Δ for $m = 0$ and $m = 4.5$ MeV at $T = 1$ keV in the cut-off regularization.

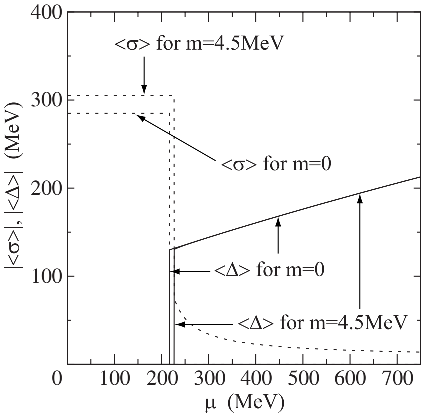

FIG. 2: Behavior of the expectation values of auxiliary fields σ and Δ for $m = 0$ and $m = 4.5$ MeV at $T = 1$ keV in the dimensional regularization.

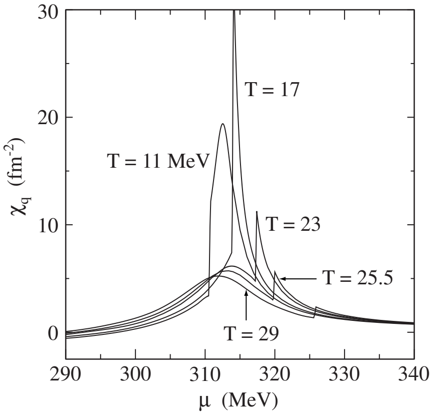

FIG. 3: Quark number susceptibility for $\mu = 11, 17, 23, 25.5,$ 29 MeV in the model with cut-off regularization.

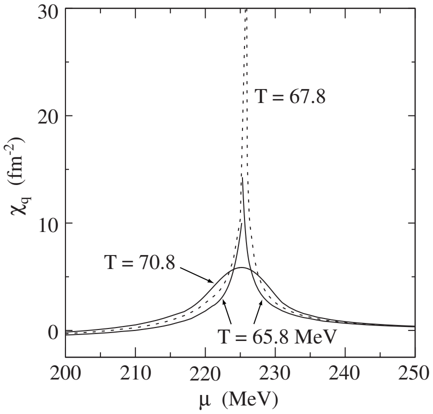

FIG. 4: Quark number susceptibility for $\mu = 65.8, 67.8, 70.8$ MeV in the model with dimensional regularization.

chemical potential μ increases. At the massless limit, the critical chemical potential for the chiral symmetry breaking is found to be $\mu \simeq 300$ and 220 MeV in the case of the cut-off and the dimensional regularizations respectively. A large mass gap is observed in Fig. 2. There is no coexistence phase with non-vanishing $\langle\sigma\rangle$ and $\langle\Delta\rangle$ in the dimensional regularization. The current quark mass hardly affects the behavior of the expectation value $\langle\Delta\rangle$. The behavior of $\langle\Delta\rangle$ in Fig. 2. is quite different from that in Fig. 1. As is clearly seen in Fig. 2, the absolute value $|\langle\Delta\rangle|$ monotonically increases as a function of μ. In the cut-off regularization, $\langle\Delta\rangle$ is suppressed near the cut-off scale, $\mu \sim \Lambda$ $(= 720$ MeV$)$.

We also calculate the quark number susceptibility χ_q [30, 31, 32, 33, 34] which is defined by

$$\chi_q \equiv -\frac{\partial}{\partial\mu} n(\langle\sigma\rangle, \langle\Delta\rangle), \tag{18}$$

where $n(\langle\sigma\rangle, \langle\Delta\rangle)$ is the quark number density,

$$\begin{aligned} n(\langle\sigma\rangle, \langle\Delta\rangle) &= \langle\psi^\dagger\psi\rangle = -\frac{\partial}{\partial\mu} V_{\text{eff}}(\langle\sigma\rangle, \langle\Delta\rangle) \\ &= \frac{\tilde{A}}{\Gamma\left(\frac{D-1}{2}\right)} \int_0^\infty dp\, p^{D-2} \\ &\quad \times \left[\frac{\xi_+}{E_+} \tanh\left(\frac{\beta E_+}{2}\right) \right. \\ &\quad \left. + \frac{1}{2} \tanh\left(\frac{\beta\xi_+}{2}\right) - (\mu \to -\mu) \right]. \end{aligned} \tag{19}$$

Figures 3 and 4 show the behavior of χ_q as a function of the chemical potential in the cut-off and the dimensional regularizations, respectively. In Fig. 3 we show the behavior of the susceptibility χ_q near the phase boundary. A coexistence phase can be realized and different critical points are observed for $\langle\sigma\rangle$ and $\langle\Delta\rangle$ in the cut-off regularization. In Fig. 3 the maximum of χ_q at $\mu \simeq 312$ MeV for $T = 29$ MeV is induced by the chiral symmetry breaking. Decreasing the temperature, moves this peak to the right until $T \sim 23$ MeV. The gap at $\mu \simeq 327$ MeV for $T = 29$ MeV is generated by the color symmetry breaking. This gap moves to the left as the temperature decreases. The susceptibility for the peak (gap) higher than that for the gap (peak), implies a crossover (the first order phase transition). The chemical potentials for the peak and the gap degenerate at $T \simeq 17$ MeV, it corresponds to the critical end point (CEP). There is a simpler behavior of χ_q in the dimensional regularization. There is no coexistence phase as is seen in Fig. 4. Such a picture is consistent with the Fig. 2.

The phase structure of the chiral $SU_L(2) \times SU_R(2)$ symmetry and 2SC in the cut-off and the dimensional regularizations are shown in the Figs. 5 and 6, respectively. We plot the boundary of the phase where χ_q has the peak or the gap for $m = 4.5$ MeV and also the boundary where $\langle\sigma\rangle$ and/or $\langle\Delta\rangle$ disappear at the massless limit, $m \to 0$. The coexistence phase induces a complex structure around the CEP in the cut-off regularization. We find the tricritical point (TCP) at $(T, \mu) = (46.7, 281)$ and CEP at $(T, \mu) = (17.0, 314)$. As is clearly seen in

Fig. 5, the 2SC is suppressed as μ approaches to the cut-off scale. In Fig. 6 we observe TCP at $(T, \mu) = (87.2, 194)$ and CEP at $(67.8,\ 226)$. In the dimensional regularization the 2SC gets enhanced as μ increases.

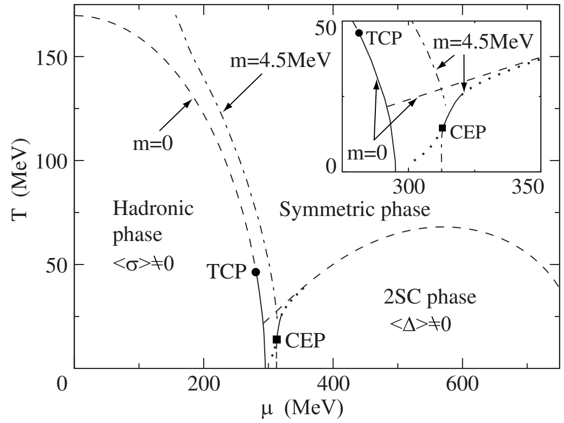

FIG. 5: Phase diagram for the model with the cut-off regularization. The solid, the dashed and the dashed-dotted lines denote the first, the second order phase transition and the crossover, respectively. We also plot the secondary maximum of χ_q by the dotted line.

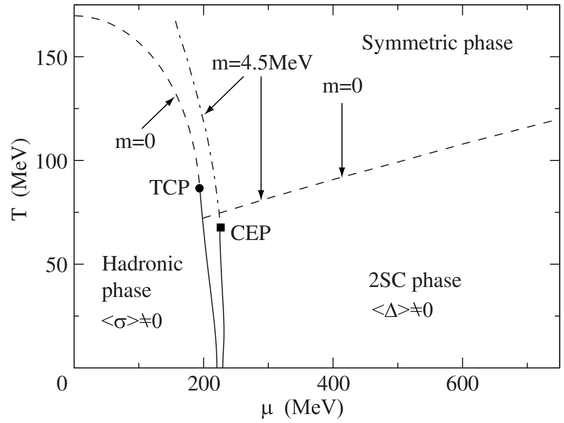

FIG. 6: Phase diagram for the model with the dimensional regularization. The solid, the dashed and the dashed-dotted lines denote the first, the second order phase transition and the crossover, respectively.

IV. ENERGY-MOMENTUM TENSOR

Here we discuss the EoS in the extended NJL model. The energy-density and the pressure of the system are given by the energy-momentum tensor. Thus we calculate the energy-momentum tensor at finite T and μ in the dimensional regularization and compare the result with that in the cut-off regularization. The energy-momentum tensor is defined by

$$\begin{aligned} \mathrm{T}_{\mu\nu} &= \frac{\partial\mathcal{L}_{\rm aux}}{\partial(\partial^{(\mu}\psi)}(\partial_{\nu)}\psi) + (\partial_{(\nu}\bar{\psi})\frac{\partial\mathcal{L}_{\rm aux}}{\partial(\partial^{\mu)}\bar{\psi})} \\ &\quad + \frac{\partial\mathcal{L}_{\rm aux}}{\partial(\partial^{(\mu}\psi^c)}(\partial_{\nu)}\psi^c) + (\partial_{(\nu}\overline{\psi^c})\frac{\partial\mathcal{L}_{\rm aux}}{\partial(\partial^{\mu)}\overline{\psi^c})} \\ &\quad - g_{\mu\nu}\mathcal{L}_{\rm aux}, \end{aligned} \tag{20}$$

where the parenthesis in the subfix indicates symmetrization,

$$A_{(\mu}B_{\nu)} = \frac{1}{2}(A_\mu B_\nu + A_\nu B_\mu).$$

Following the imaginary time formalism, we introduce the temperature and the chemical potential. We perform Wick rotation and substitute the Lagrangian density (2) into (20),

$$\begin{aligned} T_{44} &= -\frac{1}{4}\bar{\psi}\gamma_4(i\partial_4 - i\mu)\psi + \frac{1}{4}(i\partial_4 + i\mu)\bar{\psi}\gamma_4\psi \\ &\quad -\frac{1}{4}\overline{\psi^c}\gamma_4(i\partial_4 + i\mu)\psi^c + \frac{1}{4}(i\partial_4 - i\mu)\overline{\psi^c}\gamma_4\psi^c \\ &\quad +\frac{1}{2}\bar{\psi}(i\not{\partial} - i\mu\gamma_4 - \sigma - m)\psi \\ &\quad +\frac{1}{2}\overline{\psi^c}(i\not{\partial} + i\mu\gamma_4 - \sigma - m)\psi^c \\ &\quad -\frac{1}{2}\Delta(i\bar{\psi}\varepsilon\epsilon^3\gamma_5\psi^c) - \frac{1}{2}\Delta^*(i\overline{\psi^c}\varepsilon\epsilon^3\gamma_5\psi) \\ &\quad -\frac{1}{4G_S}\sigma^2 - \frac{1}{4G_D}\Delta^2, \end{aligned} \tag{21}$$

and

$$\begin{aligned} T_{ii} &= -\frac{1}{4}\bar{\psi}\gamma_i i\partial_i\psi + \frac{1}{4}i\partial_i\bar{\psi}\gamma_i\psi \\ &\quad -\frac{1}{4}\overline{\psi^c}\gamma_i i\partial_i\psi^c + \frac{1}{4}i\partial_i\overline{\psi^c}\gamma_i\psi^c \\ &\quad +\frac{1}{2}\bar{\psi}(i\not{\partial} - i\mu\gamma_4 - \sigma - m)\psi \\ &\quad +\frac{1}{2}\overline{\psi^c}(i\not{\partial} + i\mu\gamma_4 - \sigma - m)\psi^c \\ &\quad -\frac{1}{2}\Delta(i\bar{\psi}\varepsilon\epsilon^3\gamma_5\psi^c) - \frac{1}{2}\Delta^*(i\overline{\psi^c}\varepsilon\epsilon^3\gamma_5\psi) \\ &\quad -\frac{1}{4G_S}\sigma^2 - \frac{1}{4G_D}\Delta^2. \end{aligned} \tag{22}$$

To study phenomena in the static star, we take the thermal average of the energy-momentum tensor. It is given by the expectation value in the ground state where the equations of motion,

$$\begin{aligned} &\frac{1}{2}\bar{\psi}(i\not{\partial} - i\mu\gamma_4 - \sigma - m)\psi - \frac{1}{4}\Delta^*(i\overline{\psi^c}\varepsilon\epsilon^3\gamma_5\psi) \\ &-\frac{1}{4}\Delta(i\bar{\psi}\varepsilon\epsilon^3\gamma_5\psi^c) = 0, \end{aligned} \tag{23}$$

and

$$\begin{aligned} &\frac{1}{2}\overline{\psi^c}(i\not{\partial} + i\mu\gamma_4 - \sigma - m)\psi^c - \frac{1}{4}\Delta^*(i\overline{\psi^c}\varepsilon\epsilon^3\gamma_5\psi) \\ &-\frac{1}{4}\Delta(i\bar{\psi}\varepsilon\epsilon^3\gamma_5\psi^c) = 0, \end{aligned} \tag{24}$$

are satisfied. Therefore the expectation values of the stress tensor elements are simplified to

$$\begin{aligned}\langle T_{44}\rangle = \lim_{y\to x}\frac{1}{4}\mathrm{tr}\,\big[&\gamma_4(i\partial_4^x - i\mu)\langle\psi(x)\bar{\psi}(y)\rangle\\ &-(i\partial_4^y + i\mu)\gamma_4\langle\psi(x)\bar{\psi}(y)\rangle\\ &+\gamma_4(i\partial_4^x + i\mu)\langle\psi^c(x)\overline{\psi^c}(y)\rangle\\ &-(i\partial_4^y - i\mu)\gamma_4\langle\psi^c(x)\overline{\psi^c}(y)\rangle\big]\\ &-\frac{1}{4G_S}\langle\sigma\rangle^2 - \frac{1}{4G_D}\langle\Delta\rangle^2,\end{aligned}\tag{25}$$

and

$$\begin{aligned}\langle T_{ii}\rangle = \lim_{y\to x}\frac{1}{4}\mathrm{tr}\,\big[&\gamma_i i\partial_i^x\langle\psi(x)\bar{\psi}(y)\rangle - i\partial_i^y\gamma_i\langle\psi(x)\bar{\psi}(y)\rangle\\ &+\gamma_i i\partial_i^x\langle\psi^c(x)\overline{\psi^c}(y)\rangle - i\partial_i^y\gamma_i\langle\psi^c(x)\overline{\psi^c}(y)\rangle\big]\\ &-\frac{1}{4G_S}\langle\sigma\rangle^2 - \frac{1}{4G_D}\langle\Delta\rangle^2.\end{aligned}\tag{26}$$

To regularize the composite operator with the quark fields at the same point we consider quark fields at the slightly different space-time points, x and y [44, 45, 46]. The expectation values of the composite operators $\langle\psi(x)\bar{\psi}(y)\rangle$ and $\langle\psi^c(x)\overline{\psi^c}(y)\rangle$ are the diagonal matrix elements of the quark propagator in the Nambu-Gor'kov representation.

Substituting the fermion propagator obtained in Sec. II into Eqs. (25) and (26) and integrating over the angle variables, we obtain

$$\begin{aligned}\frac{\langle T_{44}\rangle}{M_0^{D-4}} = &-\frac{1}{4G_S}\langle\sigma\rangle^2 - \frac{1}{4G_D}\langle\Delta\rangle^2\\ &+\frac{\tilde{A}}{\Gamma(\frac{D-1}{2})}\int_0^\infty dp\; p^{D-2}\\ &\times\left[\frac{E_+^2-\mu\xi_+}{E_+}\tanh\left(\frac{\beta E_+}{2}\right)\right.\\ &\left.+\frac{E}{2}\tanh\left(\frac{\beta\xi_+}{2}\right) + (\mu\to-\mu)\right],\end{aligned}\tag{27}$$

and

$$\begin{aligned}\frac{\langle T_{ii}\rangle}{M_0^{D-4}} = &-\frac{1}{4G_S}\langle\sigma\rangle^2 - \frac{1}{4G_D}\langle\Delta\rangle^2\\ &-\frac{\tilde{A}}{(D-1)\Gamma\left(\frac{D-1}{2}\right)}\int_0^\infty dp\frac{p^D}{E}\\ &\times\left[\frac{\xi_+}{E_+}\tanh\left(\frac{\beta E_+}{2}\right)\right.\\ &\left.+\frac{1}{2}\tanh\left(\frac{\beta\xi_+}{2}\right) + (\mu\to-\mu)\right],\end{aligned}\tag{28}$$

where M_0 is the renormalization scale defined in the conditions (16) and (17). It should be noted that the stress tensor is renormalized to have the correct mass dimension in the four dimensional space-time. Taking the four dimensional limit and applying the modification (14), we numerically evaluate the integral in Eqs. (27) and (28) in the cut-off regularization.

Since the divergent parts of the Eqs. (27) and (28) do not depend on T and μ explicitly, we can evaluate the divergent parts in the limit, $\mu\to 0$ and $\beta\to\infty$. Using the dimensional regularization, we evaluate analytically the momentum integral. Because of the general covariance in this limit, one derives the same value for $\langle T_{44}\rangle$ and $\langle T_{ii}\rangle$,

$$\begin{aligned}\frac{\langle T_{44}\rangle_0}{M_0^{D-4}} = \frac{\langle T_{ii}\rangle_0}{M_0^{D-4}} \equiv &-\frac{1}{4G_S}\langle\sigma\rangle^2 - \frac{1}{4G_D}\langle\Delta\rangle^2\\ &-\frac{\Gamma(-\frac{D}{2})}{(2\pi)^{D/2}}\Big[2\{(\langle\sigma\rangle+m)^2+\langle\Delta\rangle^2\}^{D/2}\\ &+\{(\langle\sigma\rangle+m)^2\}^{D/2}\Big],\end{aligned}\tag{29}$$

where $\langle\sigma\rangle$ and $\langle\Delta\rangle$ depend on T and μ.

Thus we obtain a finite expression for the energy-momentum tensor

$$\begin{aligned}\frac{\langle T_{44}\rangle}{M_0^{D-4}} = &\frac{\langle T_{44}\rangle_0}{M_0^{D-4}} + \frac{\tilde{A}}{\Gamma\left(\frac{D-1}{2}\right)}\int_0^\infty dp\; p^{D-2}\\ &\times\left[\frac{E_+^2-\mu\xi_+}{E_+}\left\{\tanh\left(\frac{\beta E_+}{2}\right)-1\right\}\right.\\ &+\frac{E}{2}\left\{\tanh\left(\frac{\beta\xi_+}{2}\right)-1\right\} + (\mu\to-\mu)\\ &+(E_+ + E_- - 2\sqrt{E^2+\langle\Delta\rangle^2})\\ &\left.-\mu\left(\frac{\xi_+}{E_+}-\frac{\xi_-}{E_-}\right)\right],\end{aligned}\tag{30}$$

and

$$\begin{aligned}\frac{\langle T_{ii}\rangle}{M_0^{D-4}} = &\frac{\langle T_{ii}\rangle_0}{M_0^{D-4}} - \frac{\tilde{A}}{(D-1)\Gamma\left(\frac{D-1}{2}\right)}\int_0^\infty dp\frac{p^D}{E}\\ &\times\left[\frac{\xi_+}{E_+}\left\{\tanh\left(\frac{\beta E_+}{2}\right)-1\right\}\right.\\ &+\frac{1}{2}\left\{\tanh\left(\frac{\beta\xi_+}{2}\right)-1\right\} + (\mu\to-\mu)\\ &\left.+\left(\frac{\xi_+}{E_+}+\frac{\xi_-}{E_-}-\frac{2E}{\sqrt{E^2+\langle\Delta\rangle^2}}\right)\right].\end{aligned}\tag{31}$$

We plot the energy density, $-\langle T_{44}\rangle$, in Fig. 7 and the pressure, $\langle T_{ii}\rangle$, in Fig. 8. The origin of the energy density and pressure can not be fixed in our model. Here we set $\langle T_{44}\rangle|_{T=\mu=0}=0$ and $\langle T_{ii}\rangle|_{T=\mu=0}=0$ by hand. In 2SC phase, $\langle\Delta\rangle>0$, $-\langle T_{44}\rangle$ and $\langle T_{ii}\rangle$ monotonically increase as functions of μ. We find the equation of state from these results. It plays an essential role in the study of the structure of dense stars. As is shown in Fig. 9, there is a difference between the dimensional and the cut-off regularizations. A harder state is observed in the cut-off regularization for smaller $-\langle T_{44}\rangle$. On the other hand, a harder state is obtained in the dimensional regularization

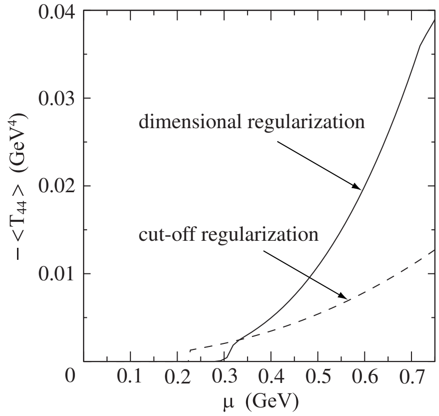

FIG. 7: Behavior of the stress tensor $-\langle T_{44}\rangle$ as functions of the chemical potential at $T = 1$ keV.

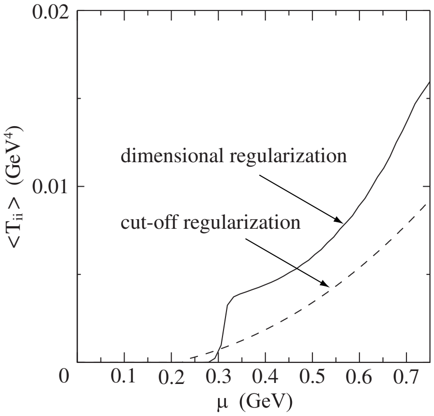

FIG. 8: Behavior of the stress tensor $\langle T_{ii}\rangle$ as functions of the chemical potential at $T = 1$ keV.

for larger $-\langle T_{44}\rangle$. It affects the core structure of dense stars with 2SC phase inside.

Next we examine the thermodynamic relationships. In the thermodynamics the energy density ρ is derived from the generating functional, Z, through the following differentiation,

$$\rho\Omega = \frac{\partial}{\partial\beta}(\ln Z) - \mu\frac{\partial}{\partial\mu}\frac{\ln Z}{\beta}. \tag{32}$$

The pressure of the system, P, is obtained by differentiating Z with respect to Ω,

$$P = \frac{\partial}{\partial\Omega}\frac{\ln Z}{\beta}. \tag{33}$$

In the present approximation for the generating functional the energy density and the pressure become

$$\rho = \frac{\partial}{\partial\beta}(\beta V_{\text{eff}}) - \mu\frac{\partial}{\partial\mu}V_{\text{eff}} \tag{34}$$

and

$$P = -V_{\text{eff}}. \tag{35}$$

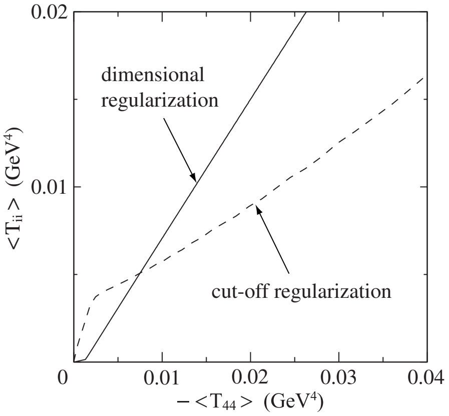

FIG. 9: Equation of state, i.e., relationship between $-\langle T_{44}\rangle$ and $\langle T_{ii}\rangle$.

First we consider the expression for the energy density. Substituting the explicit expression for the effective potential (13) into the first term of the right hand side of the Eq. (34), we get

$$\begin{aligned}\frac{\partial}{\partial\beta}(\beta V_{\text{eff}}) &= \frac{\langle\sigma\rangle^2}{4G_S} + \frac{\langle\Delta\rangle^2}{4G_D} - \frac{\tilde{A}}{\Gamma\left(\frac{D-1}{2}\right)}\int_0^\infty dp\, p^{D-2} \\ &\times\left[E_+\tanh\left(\frac{\beta E_+}{2}\right)\right. \\ &\left.+\frac{\xi_+}{2}\tanh\left(\frac{\beta\xi_+}{2}\right) + (\mu\to-\mu)\right]. \end{aligned}\tag{36}$$

The second term of the right hand side of the Eq. (34) is the number density (19), times the chemical potential μ. Therefore the energy density ρ is given by

$$\begin{aligned}\rho &= \frac{\langle\sigma\rangle^2}{4G_S} + \frac{\langle\Delta\rangle^2}{4G_D} - \frac{\tilde{A}}{\Gamma\left(\frac{D-1}{2}\right)}\int_0^\infty dp\, p^{D-2} \\ &\times\left[\frac{E_+^2-\mu\xi_+}{E_+}\tanh\left(\frac{\beta E_+}{2}\right)\right. \\ &\left.+\frac{E}{2}\tanh\left(\frac{\beta\xi_+}{2}\right) + (\mu\to-\mu)\right]. \end{aligned}\tag{37}$$

This expression exactly reproduces $-\langle T_{44}\rangle$ of the Eq. (27). Thus the time component of the stress tensor, $-\langle T_{44}\rangle$, satisfies the thermodynamic relationship for the energy density (34).

For the space component of the stress tensor, $\langle T_{ii}\rangle$, the situation is not so simple. After partial integration over p in the effective potential Eq. (13) or $\langle T_{ii}\rangle$ of the Eq. (28), we have

$$\begin{aligned}P &\simeq \langle T_{ii}\rangle + \frac{\tilde{A}}{(D-1)\Gamma\left(\frac{D-1}{2}\right)} \\ &\times\left[p^{D-1}\left(E_+ + E_- - 2\sqrt{E^2+\langle\Delta\rangle^2}\right)\right]_0^\infty \\ &\sim \langle T_{ii}\rangle + \frac{\tilde{A}\,\mu^2\langle\Delta\rangle^2}{(D-1)\Gamma\left(\frac{D-1}{2}\right)}\lim_{p\to\infty}p^{D-4}. \end{aligned}\tag{38}$$

At the limit, $p \to \infty$, P coincides with $\langle T_{ii} \rangle$ for $D < 4$. In the cut-off regularization the cut-off scale is used as the upper limit (instead of ∞) in the second term of the right hand side in Eq. (38). Since the last term has non-vanishing value, P does not coincide with $\langle T_{ii} \rangle$.

V. RADIUS AND MASS OF DENSE STAR

To see the physical implication of the regularization dependence we evaluate the radius and the mass of dense star in both the dimensional and the cut-off regularizations. For this purpose we confine ourselves to the case of a static and spherically symmetric star and do not care about the contribution of the strange quark and the neutrality of the star.

Here we numerically evaluate the TOV equations in four dimensions using the results of the previous sections. Inside the stars the gravitational force should balance the pressure of the matter. For a static and spherically symmetric star this condition is expressed by TOV equation,

$$\begin{aligned} \frac{dP(r)}{dr} &= -G\frac{\rho(r)+P(r)}{r\{r-2GM(r)\}} \\ &\quad \times\{M(r)+4\pi r^3 P(r)\}, \qquad (39) \\ \frac{dM(r)}{dr} &= 4\pi r^2 \rho(r), \qquad (40) \end{aligned}$$

where r is the radial distance from the center of a star. The pressure and the energy density are defined by the energy-momentum tensor $P(r) = \langle T_{ii} \rangle$ and $\rho(r) = -\langle T_{44} \rangle$. Because of the spherical symmetry the pressure, the energy density and the mass function $M(r)$ are given as functions of r.

We assume that the color superconducting phase can be realized inside dense stars and solve the Eqs. (39) and (40) with account of the EoS based on the extended NJL model [54]. We set the initial condition at $r = 0$ as $M(r = 0) = 0$ and $\rho(r = 0) = \rho_c$ and integrate the TOV equations. The energy density and the pressure decrease monotonically from the center to the surface. In our numerical analysis we define the surface of the quark star at the energy density, $\rho \simeq 0.0017\text{GeV}^4$, which corresponds to the ordinary energy density inside protons.

In Fig. 10 we plot the mass of a star as a function of the central energy density. For lower ρ_c the mass, M, increases with the central energy density. Increasing ρ_c, we observe the maximal value for M. The mass decreases after passing through the maximal values. No stable object can be constructed in this parameter range with a negative slope, as is shown by dotted lines in Fig. 10. The maximal value for the mass in the dimensional regularization is a few times as heavy as that in the cut-off regularization.

In Fig. 11 the mass of the star is plotted as a function of the radius r. The dotted lines correspond to the unstable solution in Fig. 10. In the dimensional regularization we obtain a heavier and a larger quark star. It means that the solution of TOV equations has a strong dependence on the regularization scheme. Since we do not include the contribution from the strange quark, our result obtained in the cut-off regularization shows a qualitatively similar behavior but does not exactly reproduce the result of the Ref. [28].

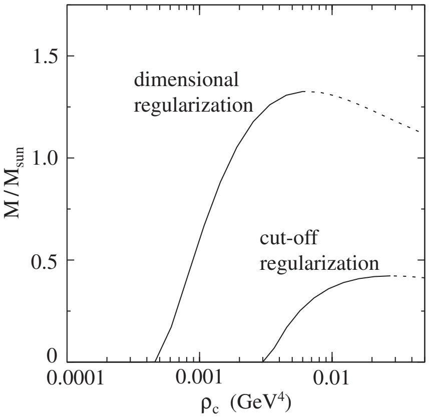

FIG. 10: Mass of the star as a function of the energy density at the center of the star. Solid and dotted lines denote the stable and unstable states respectively.

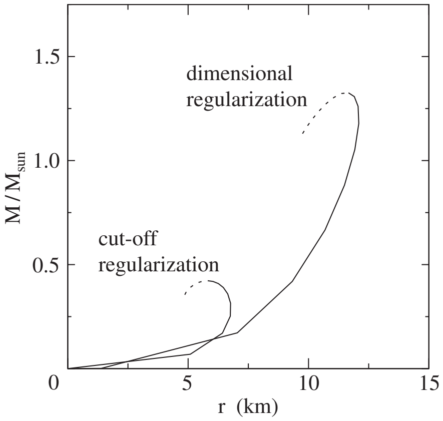

FIG. 11: Relationship between mass and radius of the star. Solid and dotted lines denote the stable and unstable states respectively.

VI. CONCLUDING REMARKS

We have investigated the phase structure of the chiral symmetry breaking and the diquark condensation ($SU_c(3)$ symmetry spontaneous breaking) on the basis of the extended two-flavor NJL model by using the dimensional and the cut-off regularizations.

Evaluating the effective potential, we obtain the expectation values of σ and Δ. The values show a different behavior for the different regularizations. In the dimensional regularization we obtain a larger mass gap and no coexistence phase with non-vanishing $\langle\sigma\rangle$ and $\langle\Delta\rangle$ at the quark massless limit, $m \to 0$. The diquark condensation, $\langle\Delta\rangle \neq 0$, is caused by the Cooper instability of quark pairs near the Fermi surface. We loose such a contribution in the cut-off regularization, as the chemical potential approaches to the cut-off scale. The diquark condensation is suppressed for a larger chemical potential, $\mu \sim \Lambda$. In the dimensional regularization $|\langle\Delta\rangle|$ monotonically increases as the chemical potential increases.

Next we studied the phase structure and the quark number susceptibility. TCP and CEP for the dimensional regularization are observed at higher temperature and lower chemical potential than those for the cut-off regularization. As is seen in Fig. 5, a complex structure is realized around CEP for the coexistence phase. It is well-known that in the framework of the perturbative QCD the 2SC is predicted even at asymptotically high values of chemical potential μ. However, one of the deficiencies of the NJL model with cutoff regularization is the absence of the 2SC phase at sufficiently high values of μ. In contrast, it is shown that in the NJL model with dimensional regularization the 2SC phase is presented in the phase diagram at rather large values of μ, and this conclusion is in agreement with perturbative QCD analysis.

The NJL model used in the paper does not describe confinement. For the future study of the confinement-deconfinement transitions we are aware of the papers where confinement is simulated in NJL by introduction of the IR cutoff (to lift up the threshold of the decay into quarks) [49, 50]. There is also another way to address confinement [51], where they just compare the binding energies per a quark for the case of diquark and nucleon clustering.

Confinement may have been relevant to our previous paper [38], where we discussed the width of sigma in the leading $1/N$ order. In this paper we claimed that the problem of the unphysical width can be fixed at the next $1/N$ order, where the decay of sigma into 2π takes place. So we hoped to fix the problem of the sigma width without even simulating confinement.

We have also evaluated the energy-momentum tensor and the EoS. The dependence on the regularization observed in the high density region is not small. As is seen in Fig. 9, the rate of $\langle T_{ii}\rangle$ and $-\langle T_{44}\rangle$ is near unity in the dimensional regularization. It has been shown that thermodynamic pressure does not coincide with the space component of the stress tensor $\langle T_{ii}\rangle$ in the cut-off regularization.

Evaluating the TOV equations, we have obtained the relationship between the mass and the radius of dense stars in both regularizations. The existence of heavier and larger quark stars is expected in the dimensional regularization. The regularization dependence is mainly generated by the difference of the mass gap in Figs. 1 and 2. The diquark condensation causes only a little contribution for the mass and radius of dense stars [28]. It should be noted that the size of the mass gap depends on the regularization parameter D. We obtain a smaller mass gap for larger dimensions [37]. However, a lower dimensional four-fermion interaction model is favored in another approach to QCD phenomena. If we adopt the ladder and the instantaneous exchange approximations and neglect momentum dependent parts of the fermion self-energy, Schwinger-Dyson equation coincides with the gap equation in the two dimensional NJL model at the leading order of $1/N$ expansion [52].

The present work is mainly restricted to the analysis of the regularization dependence of observables in the extended NJL model. To apply our result to a more realistic case of a quark star we should include the contribution of the strange quarks and take into account the electric and the color neutrality. It would be also interesting to study the masses of π and σ mesons in the 2SC phase using the dimensional regularization and to compare the results with those in the 2SC phase obtained in the extended NJL model with cut-off regularization [53]. Currently we are working on these issues.

Acknowledgments

The authors appreciate the really useful referees' comments. T. Inagaki is supported by the Ministry of Education, Science, Sports and Culture, Grant-in-Aid for Scientific Research (C), 18540276, 2008.

---

[1] D. Bailin and A. Love, Phys. Rept. **107**, 325 (1984).
[2] M. Iwasaki and T. Iwado, Phys. Lett. B **350**, 163 (1995).
[3] M. Alford, K. Rajagopal and F. Wilczek, Phys. Lett. B **422**, 247 (1998). M. Alford, K. Rajagopal and F. Wilczek, Nucl. Phys. B **537**, 443 (1999).
[4] R. Rapp, T. Schafer, E.V. Shuryak and M. Velkovsky, Phys. Rev. Lett. **81**, 53 (1998).
[5] Y. Nambu and G. Jona-Lasinio, Phys. Rev. **122**, 345 (1960), *ibid.* **124**, 246 (1961).
[6] Proc. Int. Workshop on *Compact Stars in the QCD Phase Diagram*, (Copenhagen, Aug. 2001), eConf C010815 (2002); Proc. ECT Int. Workshop on Physics of Neutron Stars Interiors (NSI00), Lect. Notes Phys. 578 (2001).
[7] M. Alford, D. Blaschke, A. Drago, T. Klahn, G. Pagliara and J. Schaffner-Bielich, Nature **445**, E7 (2007).
[8] J. R. Oppenheimer and G. M. Volkoff, Phys. Rev. **55**, 374 (1939).
[9] D. Page, M. Prakash, J.M. Lattimer, and A.W. Steiner, Phys. Rev. Lett. **85**, 2048 (2000).
[10] K. Yamaguchi, M. Iwasaki and O. Miyamura, Prog. Theor. Phys. **107**, 117 (2002).
[11] M. Alford and K. Rajagopal, JHEP **0206**, 031 (2002).
[12] A.W. Steiner, S. Reddy, and M. Prakash, Phys. Rev. D

66, 094007 (2002).

[13] I. Shovkovy, M. Hanauske, and M. Huang, Phys. Rev. D **67**, 103004 (2003).

[14] S. Banik and D. Bandyopadhyay, Phys. Rev. D **67**, 123003 (2003).

[15] D. Blaschke, F. Sandin, T. Klahn and J. Berdermann, arXiv:0807.0414 [nucl-th].

[16] W. Bentz, T. Horikawa, N. Ishii and A.W. Thomas, Nucl. Phys. A **720**, 95 (2003).

[17] S. Lawley, W. Bentz and A.W. Thomas, Nucl. Phys. Proc. Suppl. **141**, 29 (2005).

[18] P. Wang, S. Lawley, D.B. Leinweber, A.W. Thomas and A.G. Williams, Phys. Rev. C **72**, 045801 (2005).

[19] T. Klahn, D. Blaschke, F. Sandin, C. Fuchs, A. Faessler, H. Grigorian, G. Ropke and J. Trumper, Phys. Lett. B **654**, 170 (2007). D.B. Blaschke, D. GomezDumm, A.G. Grunfeld, T. Klahn and N.N. Scoccola, Phys. Rev. C **75**, 065804 (2007). D.B. Blaschke, T. Klahn, and F. Sandin, J. Phys. G **35**, 014051 (2008).

[20] P.K. Panda and H.S. Nataraj, Phys. Rev. C **73**, 025807 (2006).

[21] M. Buballa and M. Oertel, Nucl. Phys. A **703**, 770 (2002).

[22] M. Baldo, M. Buballa, F. Burgio, F. Neumann, M. Oertel, and H.J. Schulze, Phys. Lett. B **562**, 153 (2003).

[23] J.E. Horvath, G. Lugones, and J.A. de Freitas Pacheco, Int. J. Mod. Phys. D **12**, 519 (2003).

[24] G. Lugones and J.E. Horvath, Astron. Astrophys. **403**, 173 (2003).

[25] M. Alford and S. Reddy, Phys. Rev. D **67**, 074024 (2003).

[26] H. Grigorian, D. Blaschke, and D.N. Aguilera, Phys. Rev. C **69**, 065802 (2004).

[27] D. Blaschke, H. Grigorian, D.N. Aguilera, S. Yasui, and H. Toki, AIP Conf. Proc. Acoust. Phys. **660**, 209 (2003).

[28] S.B. Ruster and D.H. Rischke, Phys. Rev. D **69**, 045011 (2004)

[29] D. Blaschke, S. Fredriksson, H. Grigorian, A.M. Oztas and F. Sandin, Phys. Rev. D **72**, 065020 (2005).

[30] Y. Hatta and T. Ikeda, Phys. Rev. D **67**, 014028 (2003).

[31] B.-J. Schaefer and J. Wambach Phys. Rev. D **75**, 085015 (2007).

[32] P Costa, C.A. de Sousa, M.C. Ruivo and Yu.L. Kalinovsky Phys. Lett. B **647**, 431 (2007). P. Costa, M.C. Ruivo and C.A. de Sousa, Phys. Rev. D **77**, 096001 (2008).

[33] C. Sasaki, B. Friman and K. Redlich Phys. Rev. D **77**, 034024 (2008).

[34] K. Fukushima, Phys. Rev. D **77**, 114028 (2008).

[35] L. P. Gorkov, JETP **7**, 993 (1958), Y. Nambu, Phys. Rev. **117**, 648 (1960).

[36] T. Fujihara, T. Inagaki and D. Kimura, Prog. Theor. Phys. **117**, 139 (2007).

[37] T. Inagaki, T. Kouno and T. Muta, Int. J. Mod. Phys. A **10**, 2241 (1995).

[38] T. Inagaki, D. Kimura and A. Kvinikhidze, Phys. Rev. D **77**, 116004 (2008).

[39] S. Krewald and K. Nakayama, Annals Phys. **216**, 201 (1992).

[40] R.G. Jafarov, and V.E. Rochev, Russ. Phys. J. **49**, 364 (2006), Izv. Vuz. Fiz. **49**, 20 (2006).

[41] Y. Kikukawa and K. Yamawaki, Phys. Lett. B **234**, 497 (1990).

[42] T. Muta, *Nagoya Spring School on Dynamical Symmetry Breaking*, 3 (ed. K. Yamawaki, World Scientific, 1992).

[43] H.-J. He, Y.-P. Kuang, Q. Wang and Y.-P. Yi, Phys. Rev. D **45**, 4610 (1992).

[44] P. A. M. Dirac, Proc. Cambridge Phil. Soc. **30**, 150 (1934).

[45] R. Peierls, Proc. Roy. Soc., Series A **146**, 420 (1934).

[46] J. Schwinger, Phys. Rev. **82**, 664 (1951).

[47] N. Petropoulos, J. Phys. G **25**, 225 (1999).

[48] J. T. Lenaghan and D. H. Rischke, J. Phys. G **26**, 431 (2000).

[49] W. Bentz and A.W. Thomas, Nucl. Phys. A **696**, 138 (2001).

[50] W. Bentz, T. Horikawa, N. Ishii and A.W. Thomas Nucl. Phys. A **720**, 95 (2003).

[51] S. Pepin, M.C. Birse, J.A. McGovern and N.R. Walet, Phys. Rev. C **61**, 055209 (2000).

[52] T. Fujihara, T. Inagaki, D. Kimura and A. Kvinikhidze, Prog. Theor. Phys. Suppl. **174**, 72 (2008): arXiv:0806.1331 [hep-ph]

[53] D. Ebert, K.G. Klimenko and V.L. Yudichev, Phys. Rev. C **72**, 015201 (2005), Phys. Rev. D **72**, 056007 (2005), *ibid.* **75**, 025024 (2007).

[54] This procedure is valid until the energy density inside the star is in the deconfinement phase. Here we evaluate the structure of a quark star in which confinement phase is realized only near the surface of the star and ignore the contribution of the confinement phase.